Ab Initio Study of the Reaction of NO_3 with the OH Radical

Luminita C. Jitariu and David M. Hirst*

Department of Chemistry, University of Warwick, Coventry, CV4 7AL, U.K.

Received: May 24, 1999

The geometries of transition states and adducts have been optimized in MP2/6-311++G** calculations on both the singlet and triplet potential energy surfaces for the reaction of NO_3 with OH. Single point calculations have been made at the G2MP2 level. Reaction is shown to be most likely to occur on the singlet surface via an adduct whose structure is very similar to that of pernitric acid, HO_2NO_2. The formation of the adduct is exothermic, and the calculated enthalpy of activation is -8 kJ mol^{-1}. This adduct can dissociate to $HO_2 + NO_2$ directly or via rotational isomers. Reaction on the triplet surface is unlikely to be important because the formation of a triplet adduct has a large enthalpy of activation.

1. Introduction

The hydroxyl radical (OH) dominates the daytime oxidation chemistry in the troposphere, controlling the atmospheric lifetimes of the majority of trace species that are emitted naturally or via man's activity. Its concentration defines the oxidizing capacity of the atmosphere. The OH radical is produced *mainly* by the photolysis of ozone to form O (^{1}D) which then reacts with H_2O. This highly reactive radical has the ability to control the HO_x cycle and other species that contribute to acid rain or photochemical smog. It has been assumed for many years that there is no source for the OH at night.

Hall et al.[1] and Mellouki et al.[2] have studied the reaction of the NO_3 radical with HO_2, which could occur during the nighttime when the NO_3 radical has a stationary concentration. They showed that the channel which yields OH + NO_2 + O_2 is fast enough to ensure the conversion of HO_2 to the more reactive OH radical. We have reported previously a theoretical ab initio study[3] of this reaction and suggested a mechanism for the formation of the OH radical via oxygen-bonded intermediates formed with no activation energy for reaction on the singlet potential energy surface. Another potential source of OH in the nighttime troposphere is considered to be the reaction between CH_3O_2 and NO_3 [4] as one step in a reaction sequence which could yield a significant amount of OH. Platt et al.[5] estimated the actual concentration of OH radicals to be about 10^5 molecules cm^{-3} and concluded that the rate of OH production could be only 1 order of magnitude less by night than it is by day. The role of the NO_3 radical in the nighttime atmosphere is comparable to that of OH and NO during the day, and its importance in the initiation of oxidation chain reactions has been pointed out.

There have been few kinetic studies of the reaction

$$NO_3 + OH \rightarrow HO_2 + NO_2 \qquad \Delta H_{298} = -64 \text{ kJ mol}^{-1} \quad (1)$$

The first kinetic investigation was reported by Burrows et al.[6] in the modulated photolysis of HNO_3 at $\lambda = 254$ nm. They included reaction 1 in the mechanism they proposed so that the observed stationary concentration of NO_3 could be described properly. An estimate for the rate coefficient, assuming pseudo-first-order kinetics, was $k = (7.3 \pm 5.0) \times 10^{-11}$ cm^3 molecules^{-1} s^{-1} at 298 K. A later study by Boodaghians et al.[7] used the discharge-flow technique and gave a rate constant of $k = (2.0 \pm 0.6) \times 10^{-11}$ cm^3 molecules^{-1} s^{-1}. This value confirmed the high reactivity of NO_3 toward OH. At about the same time Mellouki et al.[2] used a similar flow method, but the radicals were detected by EPR. The kinetic results obtained agreed fully with the value of the rate constant reported by Boodaghians et al.[7] Hall et al.[1] considered indirectly reaction 1 as an additional reaction leading to the loss of NO_3 when various hydrogen containing species are present in the NO_3 + HO_2 system.

There are several possible product channels for the reaction of NO_3 with OH, and it is important to assess their relative contributions. Clearly definite mechanistic information is not available from the experimental studies. In these studies the mechanism of the reaction between NO_3 and OH was considered to be an oxygen-atom transfer from NO_3. The formation of HO_2 could result from a direct pathway or through an intermediate complex with a structure similar to that of the pernitric acid molecule (reaction 2). The decomposition of the HO_2NO_2 molecule could then yield reactive free radicals or stable species. Possible channels are presented as follows along with reaction enthalpies (at 298 K) calculated from thermodynamic data available in the JANAF tables.[8] The enthalpies of reactions 3 and 5 have been obtained by adding the excitation energies for the O_2 ($^1\Delta_g$) ← O_2 ($^3\Sigma_g^-$) and O (^{1}D) ← O (^{3}P) transitions, respectively, to the enthalpies for reactions 4 and 6. There is no experimental evidence for a complex mechanism since no studies of the temperature or pressure dependence have been made so far.

	ΔH_{298}/(kJ mol^{-1})	
$NO_3 + OH \rightarrow HO_2NO_2$	−166.1	(2)
$NO_3 + OH \rightarrow HONO(^1A') + O_2(^1\Delta_g)$	−100.2	(3)
$NO_3 + OH \rightarrow HONO + O_2(^3\Sigma_g^-)$	−191.2	(4)
$NO_3 + OH \rightarrow HONO_2 + O(^1D)$	192.3	(5)
$NO_3 + OH \rightarrow HONO_2 + O(^3P)$	+2.5	(6)

* To whom correspondence should be addressed. Fax: ++44-2476-524112. E-mail: D.M.Hirst@warwick.ac.uk.

10.1021/jp991709z CCC: $18.00
Published on Web 07/30/1999

TABLE 1: Calculated Relative Energies of Stationary Points, Reactants, and Products Obtained in G2MP2* Calculations[a] for the NO_3 + OH Reaction

species	MP2 6-311G**	QCISD(T) 6-311G**	MP2 6-311+G(3df,2p)	G2MP2*, 0 K	ZPE[b]	rel energies[c]	thermal corr[d]	G2MP2*, 298 K	*H*, 298 K
NO_3	−279.657 341	−279.670 040	−279.831 429	−279.882 838	0.016 480		0.019 868	−279.879 450	−279.878 506
OH	−75.572 896	−75.589 262	−75.617 541	−75.641 291	0.007 806		0.010 208	−75.638 889	−75.637 945
$NO_2(^2A_1)$	−204.657 019	−204.675 387	−204.781 507	−204.830 637	0.009 428		0.012 400	−204.827 665	−204.826 721
$HO_2(^2A'')$	−150.585 611	−150.614 966	−150.677 045	−150.723 589	0.013 001		0.016 012	−150.720 578	−150.719 634
				Singlet Surface					
1	−355.288 157	−355.323 961	−355.513 071	−355.597 865	0.026 010	−193.6	0.031 371	−355.592 504	−355.591 560
2	−355.288 157	−355.323 961	−355.513 071	−355.597 865	0.026 010	−193.6	0.031 371	−355.592 504	−355.591 560
3	−355.288 161	−355.323 961	−355.513 071	−355.597 865	0.026 010	−193.6	0.031 371	−355.592 504	−355.591 560
TS1	−355.195 556	−355.245 114	−355.423 314	−355.526 290	0.021 582	−5.7	0.027 506	−355.520 366	−355.519 422
TS2	−355.282 697	−355.320 202	−355.508 776	−355.595 612	0.025 669	−187.7	0.030 348	−355.590 933	−355.589 989
TS3	−355.274 454	−355.311 748	−355.498 930	−355.585 605	0.025 619	−161.4	0.030 321	−355.580 903	−355.579 959
TS4	−355.258 689	−355.284 542	−355.481 794	−355.559 261	0.023 386	−92.3	0.029 407	−355.553 240	−355.552 296
				Triplet Surface					
4	−355.140 491	−355.210 349	−355.361 278	−355.478 075	0.023 461	120.9	0.028 830	−355.472 706	−355.471 762
TS6	−355.106 359	−355.202 692	−355.323 842	−355.468 934	0.021 641	144.9	0.026 931	−355.463 644	−355.462 700
TS7	−355.123 071	−355.203 556	−355.344 326	−355.471 555	0.023 656	138.0	0.028 923	−355.466 288	−355.465 345

[a] Total energies are given in hartrees. [b] Zero-point energy corrections (E_h) calculated at the MP2/6-311++G** level and scaled by 0.8929. [c] Relative energies to reactants at 0 K in kilojoules per mole. [d] Thermal corrections scaled by 0.9195. [e] $E_{empiric}^{singlet} = -0.075E_h$; $E_{empiric}^{triplet} = -0.0704E_h$.

In this paper we present the results of a theoretical study of the reaction of OH with NO_3 in which we locate transition states for the formation of adducts on the singlet and triplet potential energy surfaces. On the basis of our calculations we conclude that a hydrogen abstraction mechanism does not occur on either of the potential energy surfaces.

2. Computational Details

The ab initio calculations have made with the Gaussian94 program[9] on a HP 9000/735 workstation and a DEC 8000 Superscalar computer at the Rutherford-Appleton Laboratory. Optimizations and frequency calculations for the NO_3/OH potential energy surface were performed at the UMP2(Fc)/6-311G** and at the UMP2(Fc)/6-311++G** levels. It has been shown that it is important to use large basis sets to obtain accurate energies for nitrogen-containing compounds.[10] A slightly modified version of the G2MP2 method[11] was used to obtain estimates of energies at a higher level of theory. We designate this modification as G2MP2* in which geometry optimizations and zero-point energies were obtained in MP2-(Fc)/6-311++G** calculations. The method requires single-point QCISD(T)/6-311G** and MP2(Fc)/6-311+G(3df,2p) calculations at the equilibrium geometries for all species involved. The QCISD(T) procedure of Pople et al.[12] implemented in Gaussian94 includes single, double, and triple excitations to correct the QCI energy.

Frequency calculations using analytic second derivatives were carried out for all reactants, products, and transition states. These calculations give the zero-point energies, thermal corrections at 298 K and the normal mode of the imaginary frequency associated with transition states. Normal mode assignments were made by animation of the modes using the Moplot 3.20 program.[13] We also performed intrinsic reaction coordinate (IRC) calculations to confirm the connections between various minima. Spin projection was not used in these calculations because the expectation values of the S^2 operator were less than 0.78 for all doublet species and 2.03 for triplets involved in the reaction, and spin contamination would appear to be unimportant.

3. Results and Discussion

The energies obtained in these calculations are reported in Table 1. The optimized geometries for all the stationary points located on the singlet and triplet surfaces are shown in Figures 1 and 2, respectively, and the overall profile of the potential energy surface is presented in Figure 3. The geometries shown in Figures 1 and 2 are those obtained in the UMP2(Fc)/6-311++G** calculations. The inclusion of diffuse functions in the basis set was found to have very little effect on the optimized geometries. The largest difference was found for transition state **TS1** for which the O(4)−O(5) distance shortened by 0.025 Å on addition of diffuse functions. For adducts **1**−**3** the N−O(4) bond length increased by 0.012−0.016 Å.

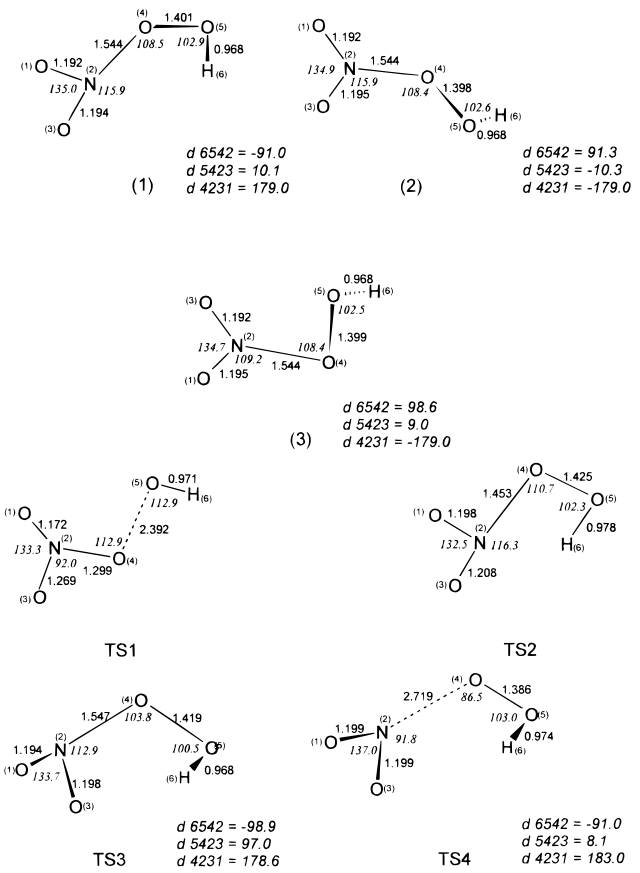

Figure 1. Stationary points located on the singlet potential energy surface (bond lengths in angstroms; bond angles (italic) in degrees) at the MP2(Fc)/6-311++G** level.

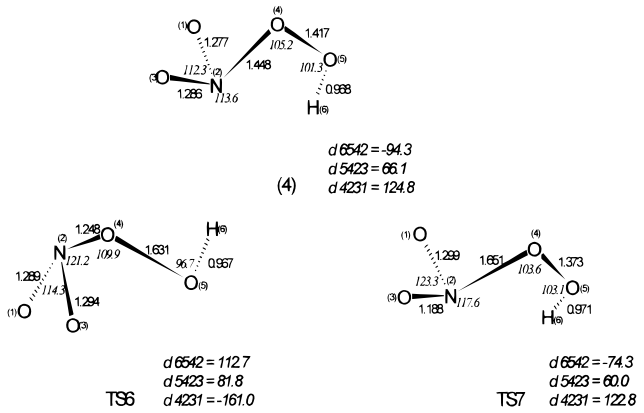

Figure 2. Stationary points located on the triplet potential energy surface (bond lengths in angstroms; bond angles (italic) in degrees) at MP2(Fc)/6-311++G** level.

3.1. Singlet Potential Energy Surface. The G2MP2* results indicate that reaction 1 is exothermic by 78.5 kJ mol^{-1}, which is only in fair agreement with the experimental value of 64.0 kJ mol^{-1}. A search for a hydrogen-bonded OH···ONO_2 adduct was performed with starting geometries corresponding to planar and slightly distorted NO_3. However, no hydrogen-bonded adduct was found at the level considered, and the NO_3 and OH moieties separated in the course of the optimization. We located three minima which are in fact rotational isomers of an O−O-bonded intermediate. Adduct **1** is more stable than the reactants by 138.5 kJ mol^{-1} at the MP2/6-311++G** level and by 193.6 kJ mol^{-1} at the G2MP2* level if zero-point energy is taken into account. The structure of adduct **1** is shown in Figure 1, and the geometric parameters indicate a structure similar to that of pernitric acid. Our optimized geometry for adduct **1** is in good agreement with that obtained by Chen and Hamilton in MP2/6-311++G(2df,2p) calculations.[14] At 298 K the formation of the adduct is exothermic by 197.2 kJ mol^{-1} at the G2MP2* level, and the calculated activation enthalpy, $\Delta H^{\ddagger}$, is −7.8 kJ mol^{-1}. This small negative enthalpy of activation is not considered to be significant because on the basis of the calculated electronic energies the transition state **TS1** lies higher than the reactants NO_3 + OH. The experimental spectroscopic data and assignment of frequencies for gas-phase HO_2NO_2 are incomplete. The first experimental study of Niki et al.[15] reported gas-phase kinetics and Fourier transform IR spectroscopy of pernitric acid. They concluded from the IR spectrum that HO_2-NO_2 was not a simple complex but a molecule with a planar or near planar structure due to internal H-bond formation. Suenram et al.[16] have reported a vibrational wavenumber of 145 cm^{-1} for torsion about the O−NO_2 bond. Further vibrational modes have been assigned in the study of aqueous HO_2NO_2 by Appelman and Gosztola.[17] An ab initio study by Saxon and Liu[18] indicated that the ground-state equilibrium geometry of HO_2-NO_2 has no symmetry and the plane of the HO_2 group lies perpendicular to that of the NO_2 moiety. A more detailed theoretical study of Chen and Hamilton[14] presented a comparison of the experimental and theoretical values for the NMR and electronic spectra, bond energies, and harmonic vibrational frequencies of pernitric acid.

Frequencies and IR intensities calculated in the present work are given in Table 2 along with the observed values, values used by Baldwin and Golden[20] in an RRKM treatment of the dissociation of HO_2NO_2, and those obtained by Saxon and Liu[18] and by Chen and Hamilton.[14] Our results from MP2 calculations are in good agreement with the available gas-phase data and support the estimated frequencies used in the RRKM calculations. The MP2/6-311++G(2df,2p) calculation of Chen and Hamilton and our calculation seem to overestimate the higher frequencies. However, Chen and Hamilton do not state whether a scaling factor has been used. Our unscaled frequencies are in good agreement with their results. The most intense transitions correspond to normal modes associated with the motion of the atoms O(3) and O(4) which form a new bond.

A transition state **TS1**, in C_s symmetry, for the formation of the adduct was located. At the MP2/6-311++G** level the negative eigenvalue of the Hessian matrix corresponds to an imaginary frequency of 499*i* cm^{-1}. An IRC calculation showed that the reaction pathway in the backward and forward directions led to reactants and adduct **1**, respectively. With analysis of the normal mode associated with the imaginary frequency, it is

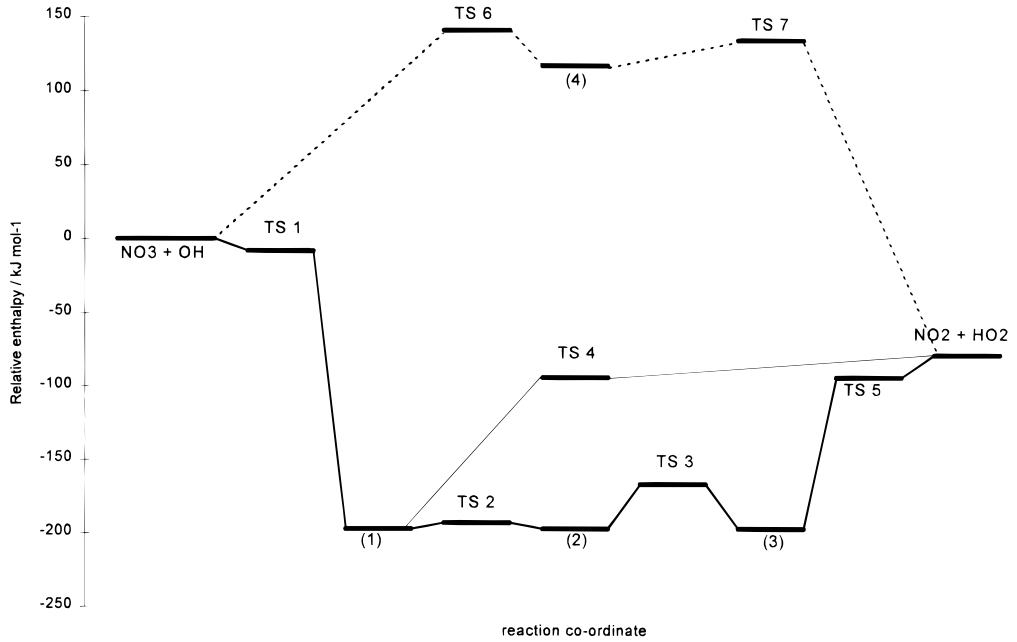

Figure 3. Overall profile of the potential energy surface for the NO_3 + OH reaction obtained in G2MP2* calculations (dotted line connects stationary points for the triplet state).

TABLE 2: Vibrational Frequencies (cm^{-1}) and Assignments for the HO_2NO_2 Intermediate on the Singlet and Triplet Surfaces

SCF 6-31G** [a]	MP2 6-311++G(2df,2pd)[b]	MP2 6-311++G** [c] singlet	rel intens	MP2 6-311++G** [c] triplet	rel intens	obsd	estd[g]	mode[h]
4100	3804	3791	52	3791	51	3540[d]		OH str
1960	1942	1951	254	1425	63	1728[d]		NO_2 asym str
1615	1445	1410	54	1252	74	1397[d]		OOH bend
1576	1326	1324	200	995	32	1304[d]		NO_2 sym str
1215	994	973	46	918	52	945[e]	880	O−O str
1046	795	786	143	656	162	803[d]		NO_2 sciss
896	753	721	6	618	3	722[e]	735	NO_2 umbrella
821	669	645	37	589	28	654[d]	633	NO(3)O(4) bend
652	457	410	89	501	4	483[e]	500	NO(3) str
436	378	356	61	378	122	340[e]	400	HOO bend
302	320	302	19	297	10		200	HOO tor
145	152	119	15	112	7	145[f]	125	O−NO_2 tor

[a] See ref 18. [b] See ref 14. [c] Unscaled frequencies calculated in this work. [d] See ref 15. [e] Aqueous HO_2NO_2, see ref 17. [f] See ref 16. [g] See ref 20. [h] Assignment done with Moplot program.

clear that the largest displacements are for O(3) in NO_3 and O(4) in the OH radical, which move together to form the new O−O bond.

Stationary points **2** and **3** are rotational isomers of **1**, about the O_2NO-OH and O_2N-OOH bonds, respectively. Interconversion of **1** and **2** occurs by internal rotation via the planar transition structure, **TS2**, with a calculated barrier of 4.1 kJ mol^{-1}. The barrier of 30.5 kJ mol^{-1} above the energy of **2** suggests that the conversion to **3** via the nonplanar transition state **TS3** will be relatively slow. Pathways for the decomposition of adducts **1** and **3** to the radicals $HO_2 + NO_2$ have also been investigated. Starting with **1** a relaxed scan of the potential energy surface was performed as the O_2N-O_2H bond was stretched. The geometry associated with the highest energy value on the potential energy surface was used as the starting point for an optimization to give a transition state **TS4**. In the UMP2/6-311++G** calculations the transition state **TS4** has a "product-like" geometry and occurs late on the potential energy surface as one would expect for an endothermic reaction. The imaginary frequency of 177*i* cm^{-1} for **TS4** indicates a loosely bound structure. The N−O(3) bond length of 2.72 Å is 1.18 Å longer than the corresponding bond in **1**. At 298 K the decomposition of isomer **3** to $HO_2 + NO_2$ is endothermic by 118.7 kJ mol^{-1}. The activation energy of 103.1 kJ mol^{-1} is close to the value of 96.3 kJ mol^{-1} used by Baldwin and Golden in their RRKM calculations.[20] The transition state for this decomposition, **TS5**, is similar to transition state **TS4**, illustrated in Figure 1, but differs in the relative orientation of the leaving fragment HO_2 which is defined by a torsion angle of −179.1°.

The decomposition of the HO_2NO_2 intermediate on the singlet potential energy surface via reactions 3 and 5 has been also investigated by scanning the surface with UMP2/6-311G** calculations, but the results did not show any possible pathways for the formation of HNO_2 or HNO_3. This conclusion is reasonable since the geometries of adduct **1** and its rotational isomers are highly unfavorable for any further internal rearrangements including hydrogen shifts. A higher order saddle point with a structure similar to the products $HNO_2 + O_2$ ($^1\Delta_g$) has been located, so we assume that in order to draw definite conclusions about the formation of these species it will be necessary to use a larger basis set or a higher level of optimization. Zhu et al.[21] demonstrated that the HO_2NO_2 molecule in the gas phase decomposes quickly into HONO and HNO_3 on the surface of the reaction vessel. The HO_2 and NO_2 radicals could possibly react to form nitrous acid. Although the formation of HONO is calculated to be thermodynamically favorable, we have found no evidence in our calculations for its formation.

The bond energies of the N−O(3) and O(3)−O(4) bonds have been computed to predict the stability of gas-phase HO_2NO_2. The calculation of the $HO-ONO_2$ and O_2N-OOH bond dissociation energies at the G2MP2* level, at 298 K, gives values of 194.7 and 116.2 kJ mol^{-1}, respectively, which compare reasonably well with the tabulated experimental[22] values of 163.2 and 96.2 kJ mol^{-1}. The values presented suggest that the unimolecular decay of pernitric acid is most likely to occur by scission of the N−O(3) bond. Our results agree well with those reported by Chen and Hamilton[14] who used the CBS-q method.[23]

3.2. Triplet Potential-Energy Surface. The triplet surface is found to be relatively simple with only three stationary points being located at the UMP2/6-311G** level. The geometries obtained in UMP2/6-311++G** calculations are presented in Figure 2. The first stationary point is adduct **4**, which has a structure similar to that of adduct **1** on the singlet surface. The NO_3 moiety becomes pyramidal with the N−O(1) and N−O(2) bonds about 0.1 Å longer than for the singlet adduct. The unscaled vibrational frequencies are reported in Table 2. One notices the lowering of the wavenumbers for the NO_2 symmetric and asymmetric stretches and for the HOO bending mode compared with the singlet adduct. The lowest frequencies are those associated with the hydroxyl oxygen atom. The O−H stretch frequency remains practically unchanged. This fact can be correlated with the geometries of adducts **1** and **4**, which show no significant difference in O−H bond length. Other than along the reaction coordinate (O−O stretch), the low-frequency vibrations are N−O−OH bending, torsion about the N−O(3) bond, and NO_2 scissor and umbrella modes. A typical heavy-atom bending frequency[24] is about 400 cm^{-1}. Our predicted values are somewhat lower, probably due to elongation of the N−O bonds. The most characteristic frequencies of the O_2NO-OH triplet complex are probably the NO_2 scissoring mode at 656 cm^{-1}, the NOO bending mode at 378 cm^{-1}, and the OOH bending mode at 1252 cm^{-1}, which are all calculated to have the highest relative intensities in the IR spectrum. A comparison with experimental frequencies for HO_2NO_2 shows that the calculated frequencies for the triplet adduct are lower by an average of about 20%.

Adduct **4** is less stable than reactants by 119.8 kJ mol^{-1} as computed at the G2MP2* level for 298 K. Calculations carried out to locate a transition state for the adduct formation successfully obtained a nonplanar transition state, **TS6**. At a temperature of 298 K the calculated thermodynamic data (at the G2MP2* level) are as follows: $\Delta H_{298} = 117.3$ kJ mol^{-1} and $\Delta H^{\ddagger} = 141.0$ kJ mol^{-1}. These results indicate that the formation of the adduct on the triplet surface would be unlikely to occur since the activation energy is so high. The value of

the imaginary frequency in the transition state has a relatively high value of $1085i$ cm^{-1}, as one would expect for a tightly bound transition state. In transition state **TS6** the NO(3) bond is elongated by 0.04 Å, while the bond being formed (O−OH) is 0.3 Å longer than in HO_2. Analysis of the eigenvector for the imaginary frequency for transition state **TS6** reveals that the reaction coordinate is given by $0.93r_{O(3)-O(4)} - 0.26r_{N-O(3)}$; i.e., the O(3)−O(4) and N−O(3) stretches make the largest contributions.

A gradient search was performed in order to locate a transition state that connects adduct **4** to the products $HO_2 + NO_2$. At the MP2 level of theory transition state **TS7** was found on the triplet surface. In the oxygen-atom abstraction transition state the length of the O−OH bond being formed is 1.37 Å (3% longer than in isolated HO_2) while the length of the O_2N-O bond being broken is 1.651 Å (33% longer than in NO_3). The calculated spin densities show that the radical character is located mainly on atom O(1) in the NO_2 group and on atom O(3) in the newly formed HO_2 radical. At the G2MP2* level we obtained an enthalpy of activation of $\Delta H^{\ddagger} = 16.8$ kJ mol^{-1} and a reaction enthalpy of $\Delta H_{298} = -195.8$ kJ mol^{-1} for the decomposition of adduct **4** to $HO_2 + NO_2$. This decomposition would be a feasible reaction pathway if adduct **4** could be formed.

4. Conclusions

In this paper we have presented ab initio calculations for the singlet and triplet potential energy surfaces for the reaction of the NO_3 radical with OH. At the level of theory employed by this study we found good agreement between our calculated values and experimental thermochemical data and bond dissociation energy. On the singlet surface an adduct is formed easily with the calculated activation enthalpy for this process being only −7.8 kJ mol^{-1}. The adduct is lower in energy than the reactants. The intermediate on the triplet surface is higher in energy than the reactants, and there is a large activation energy for its formation. For the range of temperatures which exist in the troposphere (220−300 K) reaction on the triplet surface would make only a minor contribution. The global minimum on the potential energy surface is adduct **1**, which is expected to be a long-lived intermediate which can undergo internal rotation or dissociate to $HO_2 + NO_2$. Reaction of the NO_3 radical with OH proceeds via a complicated mechanism. No evidence has been found in our calculations for a direct hydrogen-abstraction mechanism.

Acknowledgment. L.C.J. is grateful to the Foreign and Commonwealth Office for support of this research through the award of an ORS scholarship.

References and Notes

(1) Hall, I. W.; Wayne, R. P.; Cox, R. A.; Jenkin, M. E.; Hayman, G. D. *J. Phys. Chem*. **1988**, *92*, 5049.
(2) Mellouki, A.; LeBras, G.; Poulet, G. *J. Phys. Chem*. **1988**, *92*, 2229.
(3) Jitariu, L. C.; Hirst, D. M. *J. Chem. Soc., Faraday Trans*. **1998**, *94*, 1379.
(4) Biggs, P.; Canosa-Mas, C. E.; Fracheboud, J. M.; Shallcross, D. E.; Wayne, R. P. *J. Chem. Soc., Faraday Trans*. **1994**, *90*, 1205.
(5) Platt, U.; LeBras, G.; Poulet, G.; Burrows, J. P.; Moortgat, G. K. *Nature (London)* **1990**, *348*, 147.
(6) Burrows, J. P.; Tyndall, G. S.; Schneider, W.; Moortgat, G. K.; Poulet, G.; Lebras, G. *XVIIth International Conference on Photochemistry*; University of Colorado: Boulder, June 1986.
(7) Boodaghians, R. P.; Canosa-Mas, C. E.; Carpenter, P. J.; Wayne, R. P. *J. Chem. Soc., Faraday Trans. 2* **1988**, *84*, 931.
(8) Chase, M. W., Jr.; Davies, C. A.; Downey, J. R.; Frurip, D. J.; Macdonald, R. A.; Syverud, A. N. JANAF Thermochemical Tables. *J. Phys. Chem. Ref. Data Suppl*. **1985**, 14.
(9) Frisch, M. J.; Trucks, G. W.; Schlegel, H. B.; Gill, P. M. W.; Johnson, B. G.; Robb, M. A.; Cheeseman, J. R.; Keith, T. A.; Petersson, G. A.; Montgomery, J. A.; Raghavachari, K.; Al-Laham, M. A.; Zakrewski, V. G.; Ortiz, J. V.; Foresman, J. B.; Cioslowski, J.; Stefanov, B. B.; Nanayakkara, A.; Challacombe, M.; Peng, C. Y.; Ayala, P. Y.; Chen, W.; Wong, M. W.; Andres, J. L.; Replogle, E. S.; Gomperts, R.; Martin, R. L.; Fox, D. J.; Binkley, J. S.; Defrees, D. J.; Barker, J.; Stewart, J. J. P.; Head-Gordon, M.; Gonzalez C.; Pople, J. A. *Gaussian94*; Gaussian Inc.: Pittsburgh, PA, 1995.
(10) Stirling, A.; Pápai, Ì.; Mink, J.; Salahub. D. S. *J. Chem. Phys*. **1994**, *100*, 2910.
(11) Curtiss, L. A.; Raghavachari, K.; Pople, J. A. *J. Chem. Phys*. **1993**, *98*, 1293.
(12) Pople, J. A.; Head-Gordon, M.; Raghavachari, K. *J. Chem. Phys*. **1987**, ***87***, 5968.
(13) *MOPLOT Version 3.20*; Institute of Physical Chemistry, University of Fribourg: Fribourg, Switzerland, 1992.
(14) Chen, Z.; Hamilton, T. P. *J. Phys. Chem*. **1996**, *100*, 15731.
(15) Niki, H.; Marker, P. D.; Savage, C. M.; Breitenbach, L. P. *Chem. Phys. Lett*. **1977**, *45*, 564.
(16) Suenram, R. D.; Lovas, F. J.; Pickett, H. M. *J. Mol. Spectrosc*. **1986**, *116*, 406.
(17) Appelman, E. H.; Gosztola, D. J. *Inorg. Chem*. **1995**, *34*, 787.
(18) Saxon, R. P.; Liu, B. *J. Phys. Chem*. **1985**, *89*, 1227.
(19) Foresman, J. B.; Frisch, Æ. *Exploring Chemistry with Electronic Structure Methods*, 2nd ed.; Gaussian Inc.: Pittsburgh, PA, 1996.
(20) Baldwin, A. C.; Golden, D. M. *J. Phys. Chem*. **1978**, *82*, 644.
(21) Zhu, T.; Yarwood, G.; Niki, H. *Environ. Sci. Technol*. **1993**, *27*, 982.
(22) Finlayson-Pitts, B. J.; Pitts, J. N., Jr. *Atmospheric Chemistry: Fundamentals and Experimental Techniques*; Wiley: New York, 1986.
(23) Lee, C.; Yang, W.; Parr, R. G. *Phys. Rev. B* **1993**, *98*, 5648.
(24) Benson, S. W. *Thermochemical Kinetics*; Wiley: New York, 1976.